Journal of Coastal Research	SI	51	101-116	West Palm Beach, Florida	Summer 2010

Modelling the Effects of Sand Extraction, on Sediment Transport due to Tides, on the Kwinte Bank

Dries Van den Eynde[1], Alessio Giardino[2*], Jesùs Portilla[2], Michael Fettweis[1], Frederic Francken[1] and Jaak Monbaliu[2]

[1] Royal Belgian Institute of Natural Sciences
Management Unit of the North Sea
Mathematical Models
Gulledelle 100
B-1200 Brussels
Belgium
D.VandenEynde@mumm.ac.be

[2] Katholieke Universiteit Leuven
Faculty of Engineering – Civil Engineering
Department
Hydraulics Laboratory
Kasteelpark Arenberg 40
K.U.Leuven Postbus 2448
B-3001 Heverlee
Belgium

[*] Present address: Deltares
Unit Marine and Coastal Systems
Department of Morphology and Coastal
Systems,
Rotterdamseweg 185, 2600 MH, Delft
The Netherlands.

ABSTRACT

In recent years, the exploitation of marine aggregates is increasing. As an example, on the Belgian continental shelf, one particular sandbank (the Kwinte Bank) is exploited extensively; this has led to the creation of a 5 m deep depression along its central part. In the present contribution, the influence of these bathymetric changes, on erosion and sedimentation patterns are studied, using numerical modelling, in order to obtain an initial impression of the effect of such intense sand extraction on the stability of the sandbank. Different numerical models are utilised. Two-dimensional and three-dimensional hydrodynamic models have been used to derive currents, whilst third generation wave models have been used to simulate the waves. Two different models are presented, which calculate the total load sediment transport as a function of the local currents and waves. These models have been used to investigate the erosional and depositional patterns. The use of two different sediment transport models has some advantages, since the results of sediment transport models are still subject to some important uncertainties. The hydrodynamic model results are validated using ADCP current data, confirming the good performance of the models. Likewise the wave models provide good results, comparing their results with data from a buoy. The sediment transport model results were compared to the residual transport patterns, derived from the asymmetry of dunes. The results obtained seem to be in general agreement with these observations. The numerical models are used to simulate the response of the sediment transport to extensive sand extraction from the sandbank. One 'worst-case' scenario and two more realistic scenarios were simulated, whilst the effect of these bathymetric changes on sediment transport was studied. The results show that the intense sand extraction does not seem to influence extensively the stability of the sandbank, but that, as a consequence, there is less erosion and deposition. The model results show, for all of the scenarios, a small amount of deposition on the top of the sandbank; this could be an indication of a regeneration mechanism. A trench, created perpendicular to the crest of the sandbank, could be slowly refilled again. The time-scale of this regeneration and the influence of storms remain uncertain. Although the main emphasis of the paper relates to tidal forcing, a brief discussion is included on the influence of wave action, on sediment transport.

ADDITIONAL INDEX WORDS: *Sandbank, sand extraction, morphological evolution, numerical modelling, Southern North Sea*

INTRODUCTION

The demand for marine sand in Europe is increasing. In 2004, Europe produced around 53 million m³ sand and gravel of marine origin (ICES, 2005). Since 1980, the winning of marine aggregates under the Belgian jurisdiction has almost quadrupled, to about 3 million tonnes (or 1.9 million m³) each year. Up until September 2004, the extraction was undertaken in two large exploitation zones: (a) around the Thornton Bank and the Goote Bank; and (b) around the Kwinte Bank, Buitenratel and Oostdyck. More than 80 % of the extraction takes place on the Kwinte Bank, concentrated upon a small section along the northwestern and central part of the sandbank. Over the central part of the bank, this has resulted in the formation of a depression lying about 5 m below the original sea floor, about 700 m wide and 1 km long: this is the so-called Central Depression (Degrendele, Roche and Schotte, 2002).

The effects of this intense extraction of marine aggregates are only poorly known. The extraction has changed significantly the shape, volume and height of the sandbank. However, this altered morphology could also influence the current and wave patterns in the coastal waters, with possible implications on erosion of the coasts. To permit the study of the regeneration potential of the banks and the possible effects of intensive extraction on the sandbank, the depression zone was closed for exploitation (by the Government) in February 2003, for at least three years. The objective was to set-up reliable practical criteria for the maximum quantity of sand that can be extracted, without altering the long-term stability of the sandbank.

Research undertaken by Rijkswaterstaat, within the framework of the PUNAISE project, indicated that the surficial sediment structure and the bottom morphology over the exploitation zone near IJmuiden was rehabilitated after 15 months (Hoogewoning and Boers, 2001). In contrast,

DOI: 10.2112 / SI51-010.1 received 14 January 2007; accepted in revision 15 August 2008.

Rijkswaterstaat showed (within the framework of the SANDPIT project) that in a sand extraction pit near Hoek van Holland, of 10 m in depth, no clear infill was measured over a period of one year (Svašek, 2001). Elsewhere, a project undertaken by CEFAS, on the U.K. continental shelf, showed that the recovery of abandoned exploitation areas extended over 4 years or more. In Area 222 in the southern North Sea, a heavily exploited area, traces of the exploitation were still visible after 9 years (Boyd *et al*., 2004). However, the CEFAS study is on gravelly areas of the seabed.

In this contribution, numerical models are used to study the influence of sand extraction on sand transport and stability of the bank. Two different sets of models have been used. In relation to sediment transport modelling, it is useful to compare the results of different models, since these can vary over several orders of magnitude, depending upon the transport formulae used. By comparing different model results, a more balanced interpretation can be gained of the actual sediment transport.

Initially, the present situation is modelled, with the results for currents, waves and sediment transport compared to measurements, for validation purposes.

These models have been used then to examine changing patterns of currents, waves and sediment transport, in response to changes in the bathymetry of the Kwinte Bank. Three different scenarios were studied: (a) a 'worst-case', where the bank is removed at 15 m below mean sea level (MSL), *i.e.,* lowering the entire bank by more than 3 m, on average; (b) intensive sand extraction at a particular place, resulting in the generation of a trench; and (c) with the same amount of sand being extracted, but over a larger area of the Kwinte Bank, resulting in a mean deepening of the bathymetry, by almost 30 cm. The latter 2 scenarios can be used to make recommendations regarding the most suitable way to extract sand.

Initially, some general information on the Kwinte Bank is provided. Subsequently, the hydrodynamics on the Kwinte Bank are discussed. Different numerical models are then

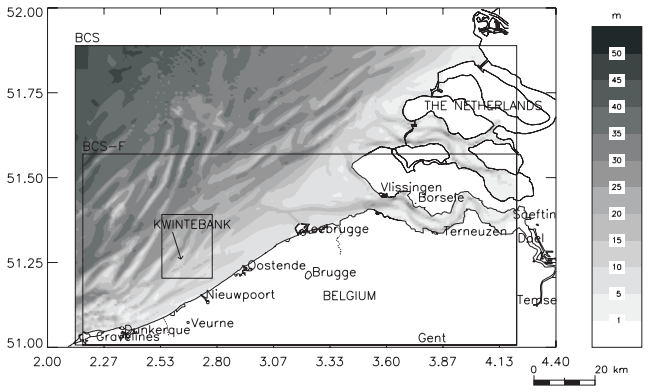

Figure 1. Bathymetry of the Belgian coastal waters. The large rectangle indicates the extension of the coarse BCS model grid, the middle-sized rectangle the extension of the fine BCS-F model grid. The smallest rectangle provides an indication of the location of the Kwinte Bank.

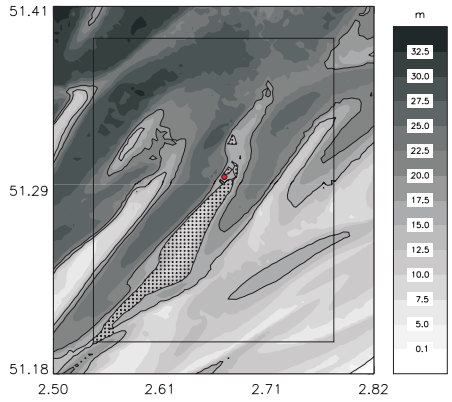

Figure 2. Detailed bathymetry (relative to MSL) of the Kwinte Bank. The rectangle is the area over which the model results are presented. The area shaded with small dots indicate the grid cells that are considered part of the Kwinte Bank and that have a depth less then 15 m with respect to MSL. The larger dot gives the location of the Central Depression (see text). Bathymetric contours are shown for 15 m and 20 m, below MSL.

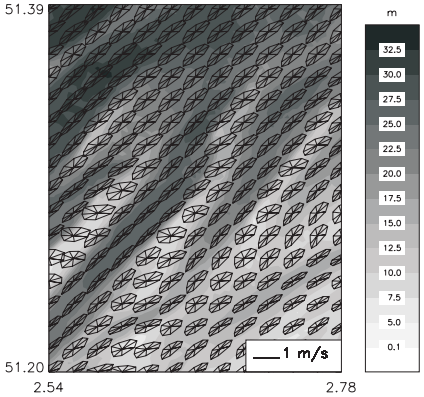

Figure 3. The bathymetry (relative to MSL) and current ellipses along the Kwinte Bank.

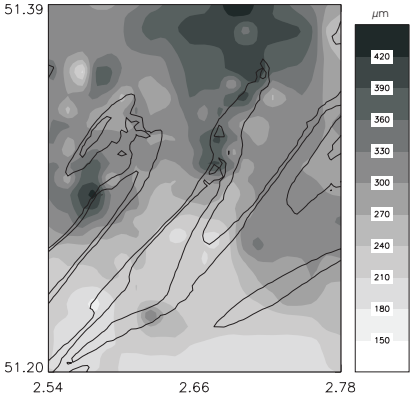

Figure 4. Median grain size of the Kwinte Bank, as used in the MU-SEDIM model. Bathymetric contours are shown for 15 m and 20 m, below MSL.

presented briefly, whilst validation of the model results is discussed. Following a description of 2 sediment transport models, their results (tide-only) are compared in relation to sediment transport pathways, derived from dune asymmetries. Likewise, the results of the numerical models for the three different scenarios are discussed, whilst wave influence on sediment transport is briefly addressed.

BACKGROUND INFORMATION

The Kwinte Bank is one of the Flemish Banks, located on the Belgian continental shelf (Figure 1). The bank is generated by tidal currents off the Belgian coast and is oriented in a SW-NE direction. The bank has a length of about 15 km, with a width varying from 2 km in its southern part, to 1 km in its northern part (Figure 2). The minimum water depth lies close to 7.5 m below MSL. Over the northern part, large dunes are present, with a maximum amplitude of around 8 m. Sand dunes are present also over the middle part of the bank; these can reach 2.5 m in height. The cross-section of the bank is clearly asymmetrical, with the steeper side facing towards the northwest.

The depth-averaged current ellipses over the Kwinte Bank region (Figure 3) typically vary depending upon their location, *i.e.,* in the swale or on the top of the sandbank. The ellipses are more spherical on the sandbanks, than in the deeper swales between the sandbanks. In the swales, the major axes of the ellipses lie nearly in the same direction as the swale/sandbank axis. However, on the sandbank, the major ellipse axes are rotated clockwise, in comparison to the bank axis. The maximum currents are around 0.9 to 1.0 m/s, on the top and the western side of the Kwinte Bank during a spring tide; they are around 0.4 to 0.5 m/s, during a neap tide.

The Kwinte Bank is characterized by fine to medium-sized sand (Figure 4). Over the southern part of the bank, sand of 180 to 240 μm is found; over the middle and the northern part, coarser sediment (of up to about 400 μm) is found. The Figure was derived on the basis of samples collected over the area, acquired by different institutes and obtained from the Belgian Marine Data Centre (BMDC). A method based upon weighted distance was used to interpolate the values for the model grid (Fettweis and Van den Eynde, 2000).

HYDRODYNAMICS

Hydrodynamic Models

Model BCS-F

The three-dimensional hydrodynamic model COHERENS (Luyten *et al.*, 1999) calculates currents and water elevations under the influence of the tides and the prevailing atmospheric conditions. This model was developed, between 1990 and 1998, within the framework of the EU-MAST projects PROFILE, NOMADS and COHERENS. The hydrodynamic model solves the momentum and continuity equations, using the 'mode-splitting' technique. COHERENS has different turbulence schemes, including the two-equation k-ε turbulence model, as used in the present study. The description of turbulence is important, when simulating the vertical current profile.

The model is implemented on the basis of two coupled grids. The coarse grid model BCS has a resolution of 42.86" in longitude (817 – 833 m) and of 25" in latitude (772 m); it has 20 layers, equally spaced over the vertical. This model provides the open sea boundaries for the fine grid BCS-F model, which has a three times higher resolution, *i.e.,* a resolution of about 275 m to 257 m, and 10 equally spaced layers over the vertical. The extension of both of the models is shown in Figure 1. On its open sea boundaries, the BCS model is coupled with two regional models. The CSM model encompasses the Northwest European Continental Shelf and calculates boundary conditions for the North Sea model (NOS). The NOS model generates boundary conditions for the BCS model. The CSM model runs in two dimensions and is driven by the elevation at the open boundaries, governed by four semi-diurnal and four diurnal harmonic constituents (Q_1, O_1, P_1, K_1, N_2, M_2, S_2, K_2). The NOS model runs in all three dimensions. All of the hydrodynamic models can take atmospheric influences into account.

Atmospheric data (wind speed, at 10 m height above sea level, together with atmospheric pressure) were obtained from the United Kingdom Meteorological Office. The data are available at a 6 h interval, on a 1.25° latitude/longitude grid. A spatial interpolation was then performed, to obtain them for the computational mesh. A linear interpolation, over time, was undertaken to calculate wind speed and pressure at each time step (Van den Eynde, Scory, and Malisse, 1995).

The BCS model was validated extensively using about 400 hours of current profiles; these were collected in the Belgian coastal zone, using a bottom-mounted Acoustic Doppler Current Profiler (ADCP), Sentinel 1200 kHz Workhorse type, from RDInstruments (Pison and Ozer, 2005, Van Lancker *et al.*, 2004). Statistical calculations (root-mean-square-error (RMSE), bias, correlation) were carried out in order to establish differences in magnitude and direction of the currents, between the model simulation results and the ADCP measurements. The RMSE of the amplitude of the currents was generally around 0.05 and 0.15 m/s, representing an relative error of about 10 % to 15 %; this varied only slightly, with depth. The error on the current direction was usually less than 20°. Thus, the validation exercise leads to the conclusion that the magnitude and direction of the current profiles are well represented by the three-dimensional hydrodynamic model.

Model TELEMAC-2D

The two-dimensional finite element hydrodynamic model TELEMAC-2D (v. 5.5) (Hervouet and Bates, 2000) was implemented on a mesh which was constructed using four different bathymetries. The large scale topography was taken from the Northeast Atlantic model, developed by Flather (1981) covering the region from 47°50'N to 71°10'N, and from 12°15'W to 12°15'E. Two intermediate bathymetries were extracted from sea-charts and corrected by Yu *et al.* (1990). The high-resolution bathymetry corresponds to the fine model BCS-F (see above). Based upon these data sets, a computational mesh was established with a node distance ranging between 70 km and 150 m on the Kwinte Bank.

At the open boundary, tidal elevation has been used as the only external forcing of the model. The same 8 constituents as for the CSM model (see above) represented the tidal forcing of the modelled region. The same atmospheric forcing was used as for the BCS-F model. A description of the model implementation is given in Giardino and Monbaliu (2004).

Table 1. *Measurements undertaken at the Kwinte Bank, with bottom-mounted ADCP. Key: Lat. - latitude in degrees North; Lon. - longitude in degrees East; Dep. - water depth referred to MSL; Dur. - duration of the measurements; Pres. - mean atmospheric pressure; and Wsp. - mean wind speed.*

Campaign	Lat.	Lon.	Dep.	Start	Dur.	Pres. (mbar)	Wsp. (m/s)
2003/15	51°18.144'	2°40.24'	16.3	11/06/03 16h30	25 h	1020	2.85
2004/04-05	5°18.151'	2°40.245'	16.3	02/03/04 12h45	216 h	1025	5.27

Table 2. *RMSE of the U-component (RMSE U), RMSE of the V-component (RMSE V) and RMSE of the norm of the depth-averaged current (RMSE C) for the BCS-F and the TELEMAC-2D model.*

		BCS-F			TELEMAC-2D		
Campaign	#	RMSE U (m/s)	RMSE V (m/s)	RMSE C (m/s)	RMSE U (m/s)	RMSE V (m/s)	RMSE C (m/s)
2003/15	39	0.140	0.119	0.127	0.279	0.145	0.215
2004/04-05	421	0.069	0.083	0.072	0.173	0.089	0.154

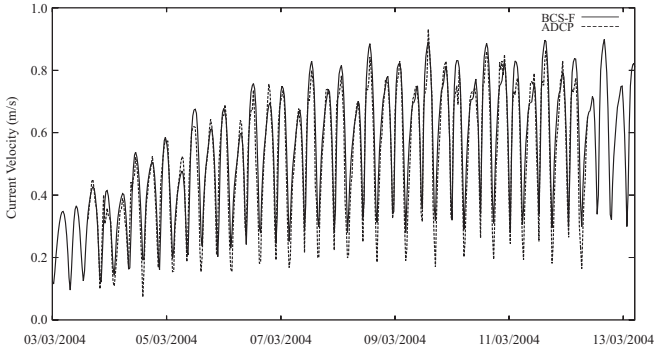

Figure 5. Measured (ADCP) and modelled (BCS-F) depth-averaged currents for the campaign 2004/04-05 on the Kwinte Bank (2°40.245' E, 51°18.151' N).

Validation on the Kwinte Bank

During two R.V. *Belgica* campaigns, measurements were undertaken on the Kwinte Bank with a bottom-mounted Acoustic Doppler Current Profiler (ADCP), Sentinel 1200 kHz Workhorse type, from RDInstruments. The sampling interval was set at 300 s. The profiles were taken with a vertical resolution of 0.5 m, with a maximum of 30 measurements over the profile. The first campaign covered a period of only a single day; however, during the second, measurements were made over a 9 day period. Calm weather conditions occurred during both periods, with mean wind speeds of 2,85 m/s (2 Bft.) and 5.27 m/s (3 Bft.) during the first and second campaigns respectively. More information on the position and timing of the measurements is listed in Table 1.

The two periods have been simulated with the BCS-F and the TELEMAC-2D model and compared with the available ADCP measurements. As an example, the depth-averaged

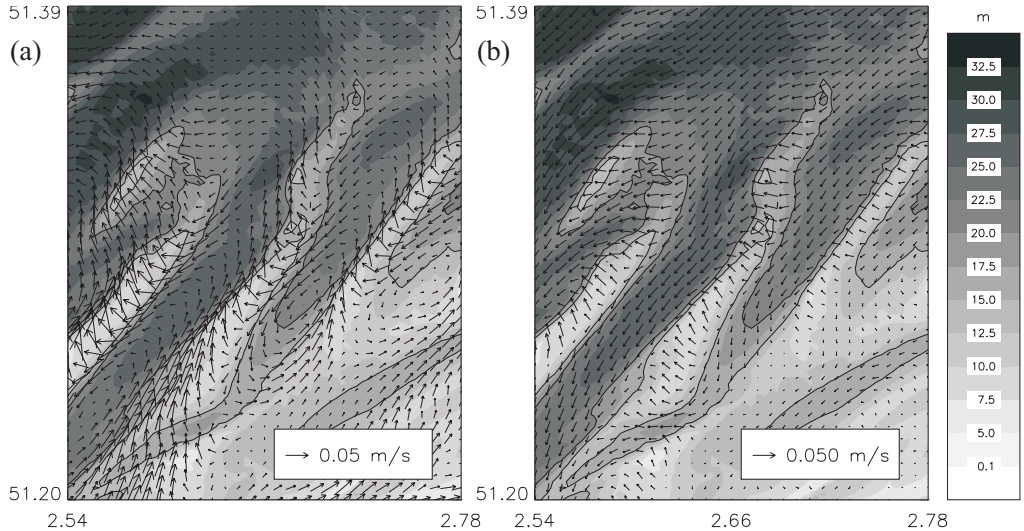

Figure 6. Tidally-induced residual currents on the Kwinte Bank for the period March 2nd 2004 6h30 – March 17th 2004 0h00, *i.e.*, a spring-neap cycle. In the background the bathymetry is shown. (a) Results of BCS-F, with one vector for each four grid points shown. (b) Results of the TELEMAC-2D model, with the results being on the same grid as the BCS-F model. Bathymetric contours are shown for 15 m and 20 m, below MSL.

current speeds for the 2004/04-05 campaigns, as modelled with the BCS-F model, together with the ADCP measurements, are presented in Figure 5.

The root-mean-square-errors (RMSE) are presented in Table 2. For the March 2004 period, the RMSE of the magnitude of the depth-averaged currents calculated by the BCS-F model is around 0.072 m/s, which is clearly satisfying. The higher RMSE for the TELEMAC-2D model are the result of a small time shift in the results, especially for the U-component of the depth-averaged current. When only taking the minima and the maxima of the depth-averaged currents into account, the RMSE for the TELEMAC-2D model are much smaller, around 0.05 m/s for the U- and the V-component for the 2004/04-05 campaigns.

Residual Currents

Both models were used to calculate the depth-averaged residual currents, during a spring-neap tidal cycle (14.8 days). The depth-averaged residual currents are defined as the vectorial mean of the depth-averaged currents at the grid points of the model over a period:

$$\overrightarrow{u_{res}} = \frac{\sum_{n} \vec{u}}{n} \qquad (1)$$

with $\overrightarrow{u_{res}}$ the depth-averaged residual current, $\vec{u}$ the depth-averaged current and n the number of depth-averaged currents, used in the derivation. The results of the BCS-F and the TELEMAC-2D model are presented in Figure 6.

The residual currents, calculated by the BCS-F model (Figure 6a) show anti-clockwise gyres centred in the swales near the sandbanks. On the western flank of the Kwinte Bank, the residual currents follow the bank towards the northeast (flood-direction); on the eastern flank, they are in the opposite direction, *i.e.*, to the southwest, in the ebb-direction. At the northern crest of the bank and in the Central Depression, the residual currents lie perpendicular to the bank crest and are ebb-dominated, flowing towards the west. The residual currents, calculated by the TELEMAC-2D model (Figure 6b) show a more uniform residual current pattern with residuals, over the bank, to the northwest.

SEDIMENT TRANSPORT DUE TO TIDES

Sediment Transport Models

Model MU-SEDIM

The sediment transport model MU-SEDIM has been implemented on the same grid as the hydrodynamic model BCS-F; it calculates the total sediment load under the influence of the local hydrodynamic conditions.

The current bottom stress, an important driving force, is a function of the depth-averaged current velocity and of the Nikuradse bottom roughness. For the calculation of the Nikuradse bottom roughness, a distinction has to be made between the skin friction and the total friction. The skin friction is the roughness, experienced by the sediments at the bottom. In this model, the expression of Engelund and Hansen (1967) has been used to calculate the skin bottom roughness.

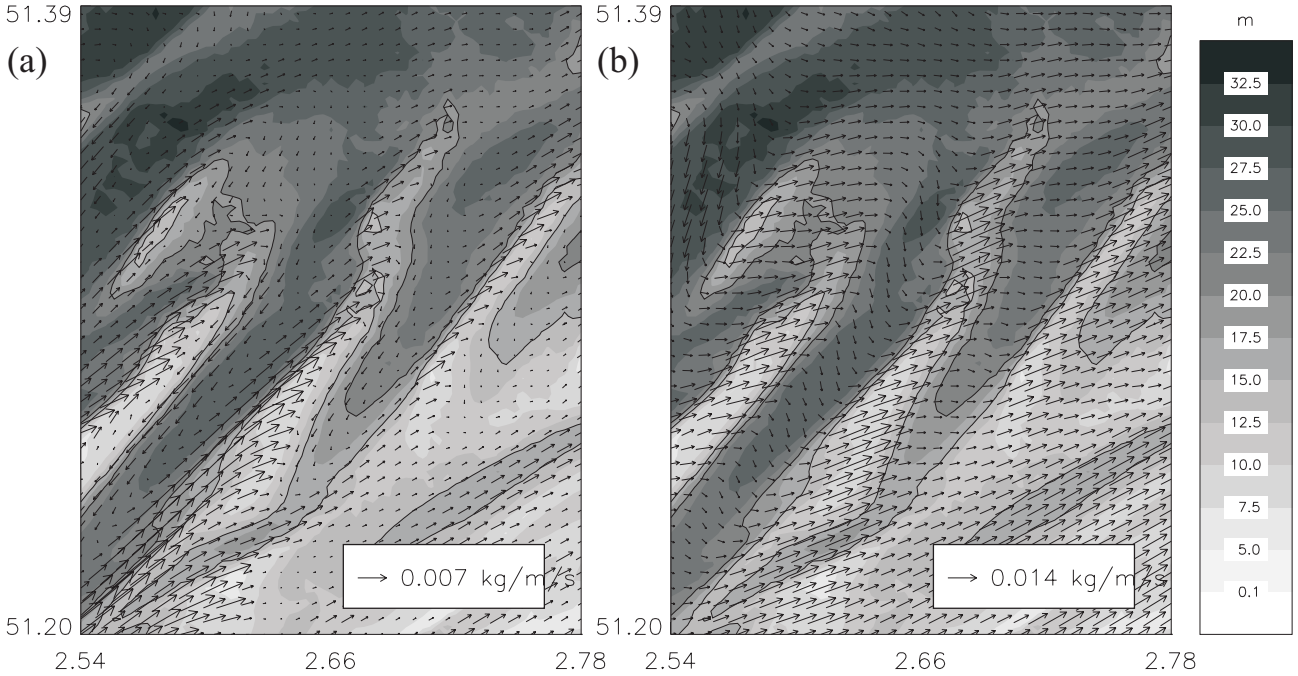

Figure 7. Tidally-induced sediment transport on the Kwinte Bank for the period March 2nd 2004 6h30 – March 17th 2004 0h00. In the background the bathymetry is shown. (a) Results of MU-SEDIM, with one vector for each four grid points shown. (b) Results of the SISYPHE model, with the results being on the same grid as the MU-SEDIM model. Bathymetric contours are shown for 15 m and 20 m, below MSL.

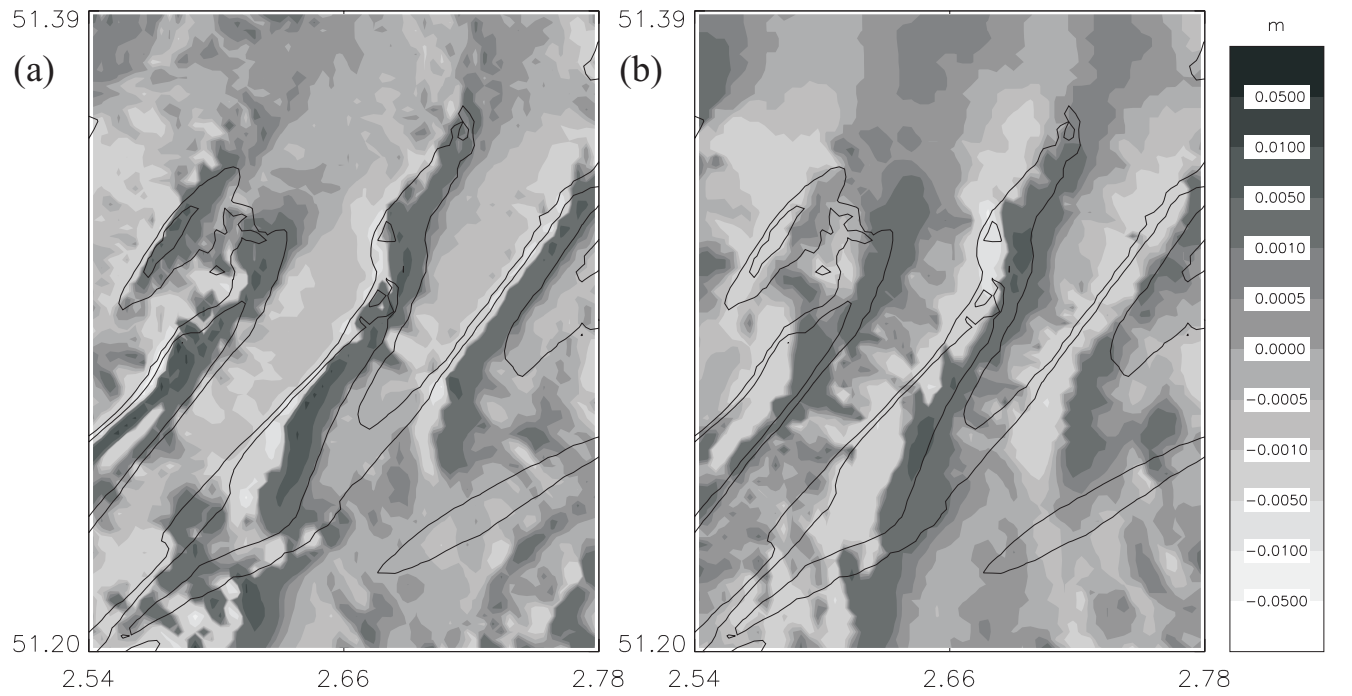

Figure 8. Erosion (light) and sedimentation (dark) patterns on the Kwinte Bank as simulated with tides only and for the period March 2nd 2004 6h30 – March 17th 2004 0h00. (a) Results of the MU-SEDIM model. (b) Results of the SISYPHE model. Bathymetric contours are shown for 15 m and 20 m, below MSL.

The total friction, on the other hand, is the friction felt by the currents and is influenced by the bed load and by the presence of bed forms. The calculation of these influences, including the calculation of the bed form dimensions, is based upon the formulae of Grant and Madsen (1982).

From the different formulae available for the prediction of sediment transport, that of Ackers and White (1973) is used here; this provided the best results, in a comparison carried out by Sleath (1984). This equation can be written as:

$$\overrightarrow{Q_s} = \vec{u} D_{35} \left(\frac{u}{u_*} \right)^n C_1 \left(\frac{F - A}{A} \right)^m \quad (2)$$

$$u_* = \sqrt{\frac{\tau}{\rho}} \quad (3)$$

where $\overrightarrow{Q_s}$ is the total transport, D_{35} the sediment diameter for which 35 % is finer, u_* the friction velocity, τ the bottom stress, ρ the water density, n, m, C_1 dimensionless parameters, F the sediment mobility number and A the critical sediment mobility number, for the commencement of transport. The sediment mobility number F can be determined using:

$$F = \left(\frac{u}{5.66 \log \frac{10h}{D_{35}}} \right)^{1-n} \frac{u_*^n}{\left((s-1) g D_{35} \right)^{1/2}} \quad (4)$$

with h the water depth, s the relative density of sediment and g the acceleration due to gravity. More details on the equations implemented in the MU-SEDIM model can be found in Van den Eynde and Ozer (1993).

The median grain-size, which is an input parameter of the sediment transport model, has been taken from the map presented as Figure 4. The D_{35} was calculated assuming a constant ratio of 0.82 between the D_{35} and the D_{50} (Cooreman *et al.*, 2000). Finally, the model calculates the morphological evolution of the sea bed, using a continuity equation for the bottom sediments (Djenidi and Ronday, 1992):

$$\rho_s (1-p) \frac{\partial \xi}{\partial t} + \nabla \overrightarrow{Q_s} = 0 \quad (5)$$

with ρ_s the sediment density, p the porosity, t time, ξ the position of the bottom, with reference to its original position, and $\nabla \overrightarrow{Q_s}$ the divergence of the sediment transport vector.

The MU-SEDIM model has already been applied at the kink of the Westhinder Bank, a sandbank at the Belgian continental shelf, north of the Kwinte Bank (Deleu *et al.*, 2004) and the model results agreed well with the transport pathways, derived from the observations, *e.g.*, from the asymmetry of the sand dunes.

Model SISYPHE

The morphodynamical model SISYPHE (v.5.5) (Villaret, 2004) was set-up on the same computational mesh as used for the TELEMAC-2D computation. The total load sand transport rate was calculated as a function of the hydrodynamic conditions, through internal coupling with the TELEMAC-

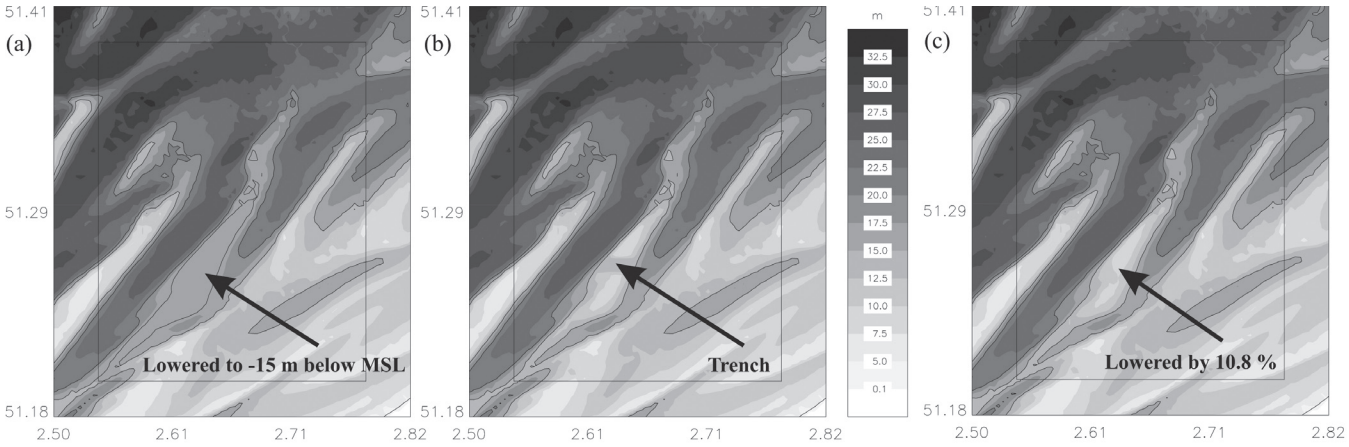

Figure 9. Bathymetry of the Kwinte Bank for the three Scenarios investigated. The lines shown are the 15 and the 20 depth contours of the original bathymetry (Figure 2); (a) Scenario 1, where the complete bank has been deepened up to 15 m below MSL; (b) Scenario 2, where a trench was cut to 13 m below MSL; and (c) Scenario 3, with a decrease in the sandbank height above 15 m below MSL by 10.8 %.

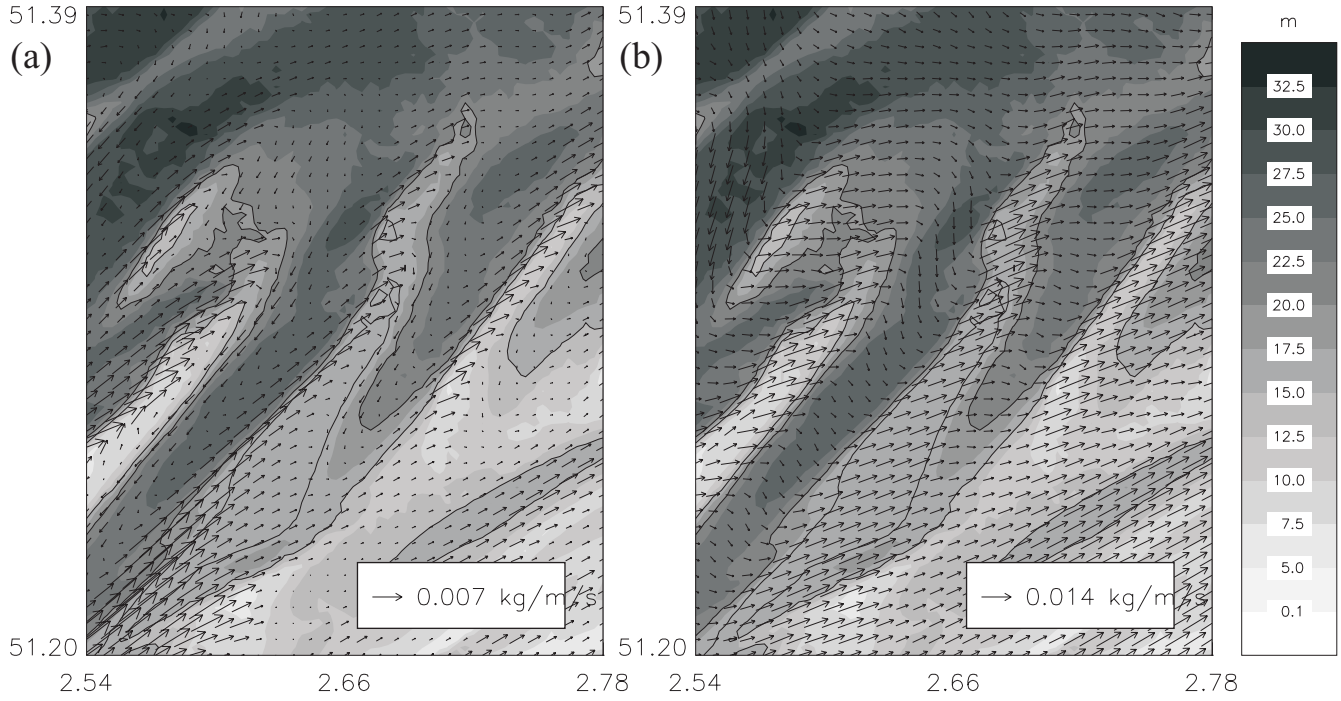

Figure 10. Predicted tidally-induced sediment transport on the Kwinte Bank for the period March 2nd 2004 6h30 – March 17th 2004 0h00 for Scenario 1, where the complete bank has been deepened up to 15 m below MSL. In the background the bathymetry is shown. (a) Results of MU-SEDIM, with one vector for each four grid points shown. (b) Results of the SISYPHE model, with the results being on the same grid as the MU-SEDIM model. Bathymetric contours are the 15 m and the 20 m depth contours, below MSL, of the original bathymetry (Figure 2).

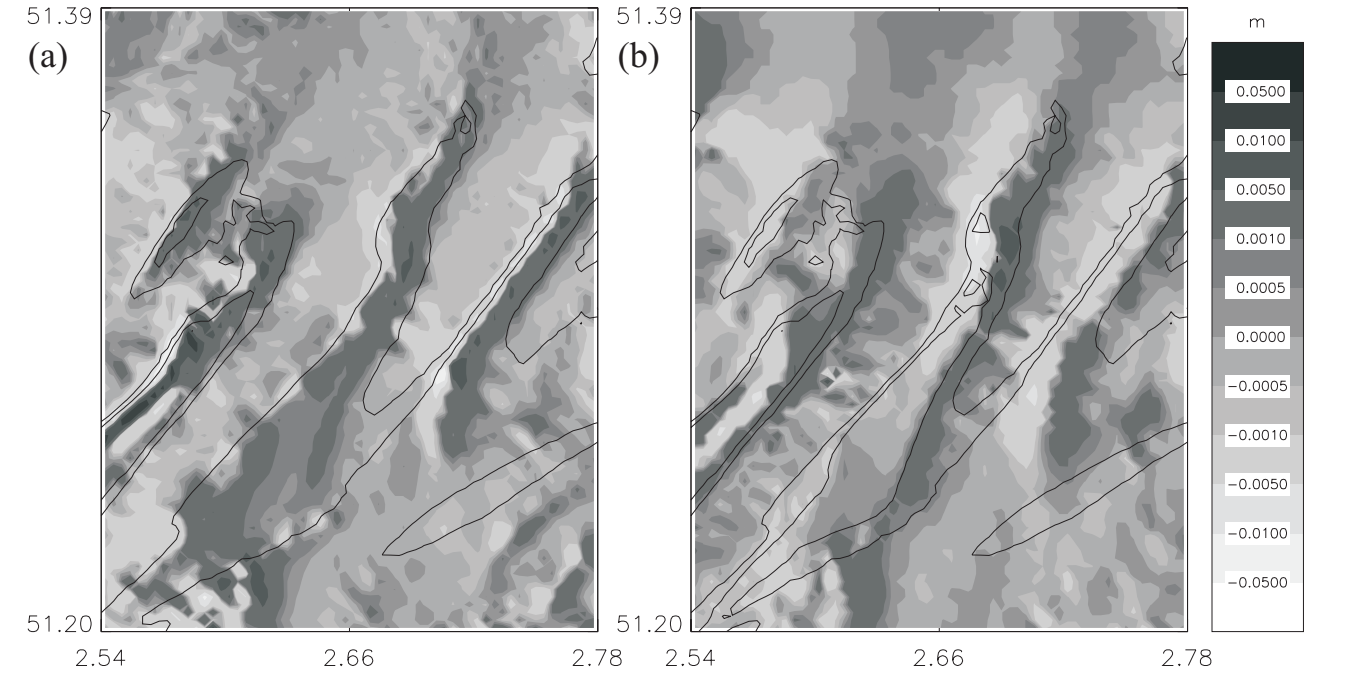

Figure 11. Erosion (light) and sedimentation (dark) patterns on the Kwinte Bank as simulated with tides only, for the period March 2nd 2004 6h30 – March 17th 2004 0h00 and for Scenario 1, where the complete bank has been deepened up to 15 m below MSL. (a) Results of the MU-SEDIM model. (b) Results of the SISYPHE model. Bathymetric contours are shown for 15 m and 20 m below MSL.

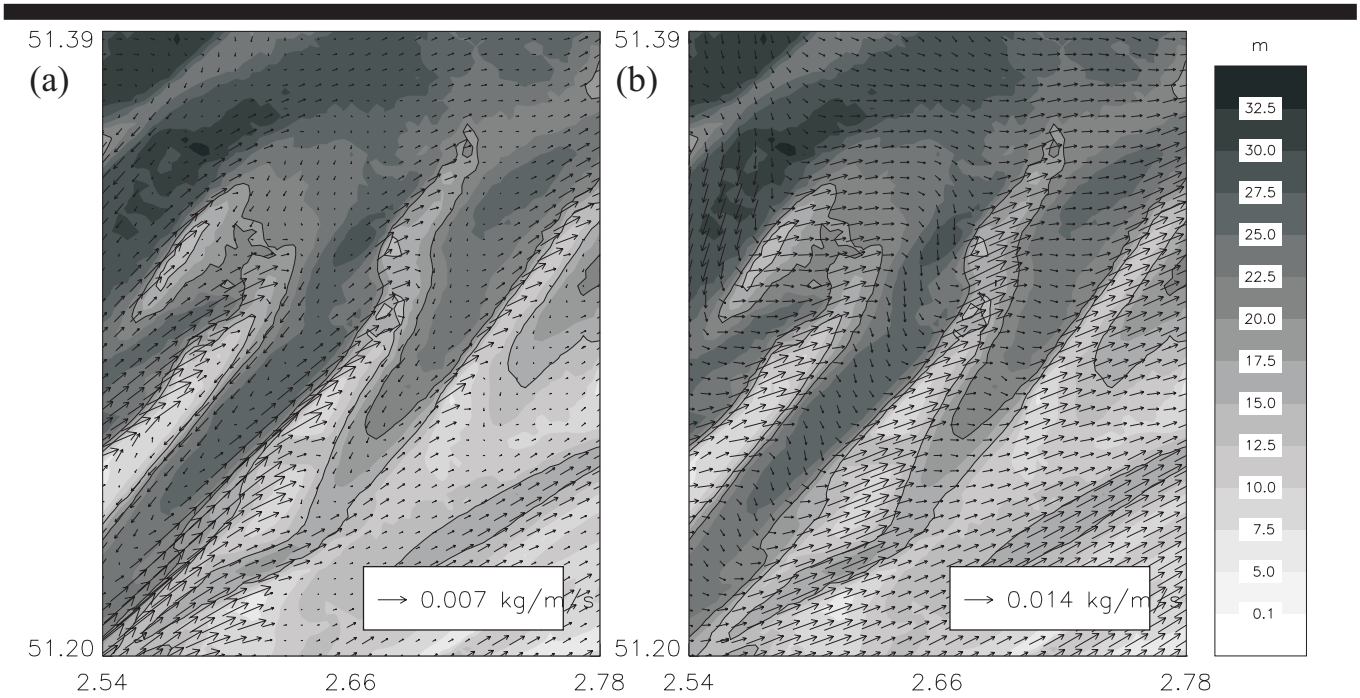

Figure 12. Predicted tidally-induced sediment transport on the Kwinte Bank for the period March 2nd 2004 6h30 – March 17th 2004 0h00 for Scenario 2, where a trench was cut to 13 m below MSL. In the background, the bathymetry is shown. (a) Results of MU-SEDIM, with one vector for each four grid points shown. (b) Results of the SISYPHE model, with the results being on the same grid as the MU-SEDIM model. Bathymetric contours are the 15 m and the 20 m depth contours, below MSL, of the original bathymetry (Figure 2).

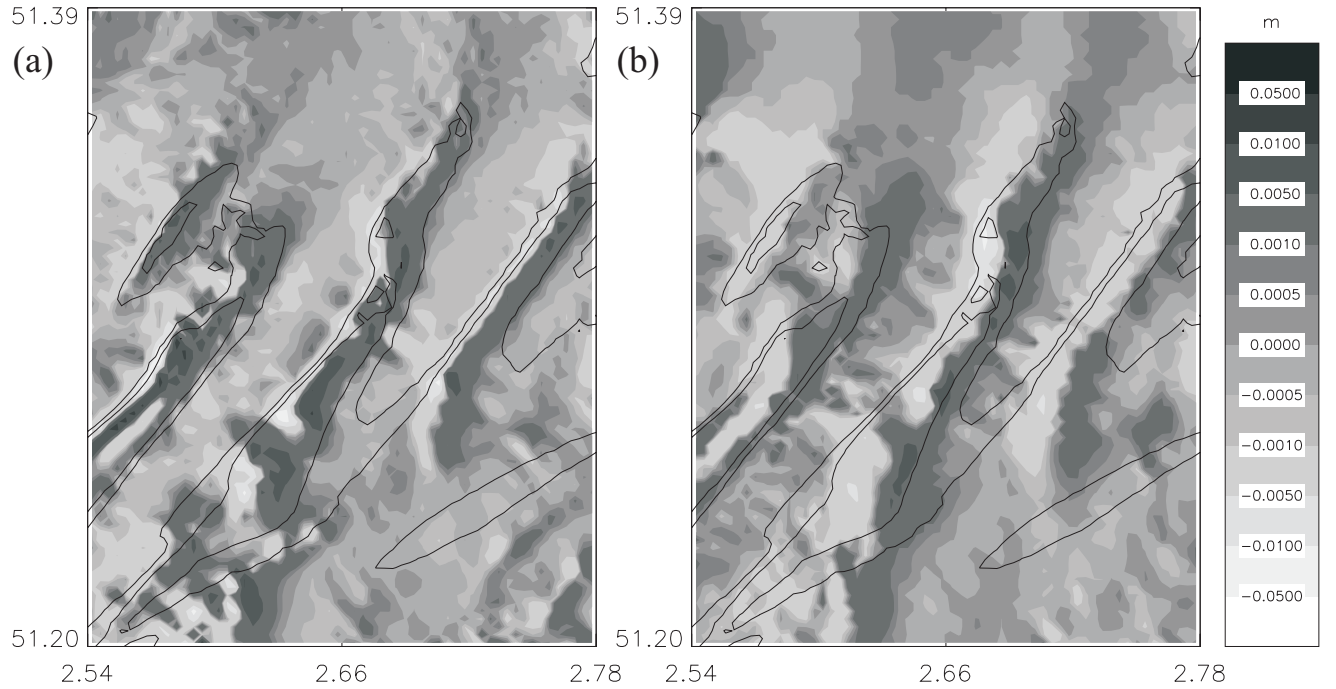

Figure 13. Erosion (light) and sedimentation (dark) patterns over the Kwinte Bank as simulated with tides only, for the period March 2nd 2004 6h30 – March 17th 2004 0h00 and for Scenario 2, where a trench was cut to 13 m below MSL. (a) Results of the MU-SEDIM model. (b) Results of the SISYPHE model. Bathymetric contours are shown for 15 m and 20 m below MSL.

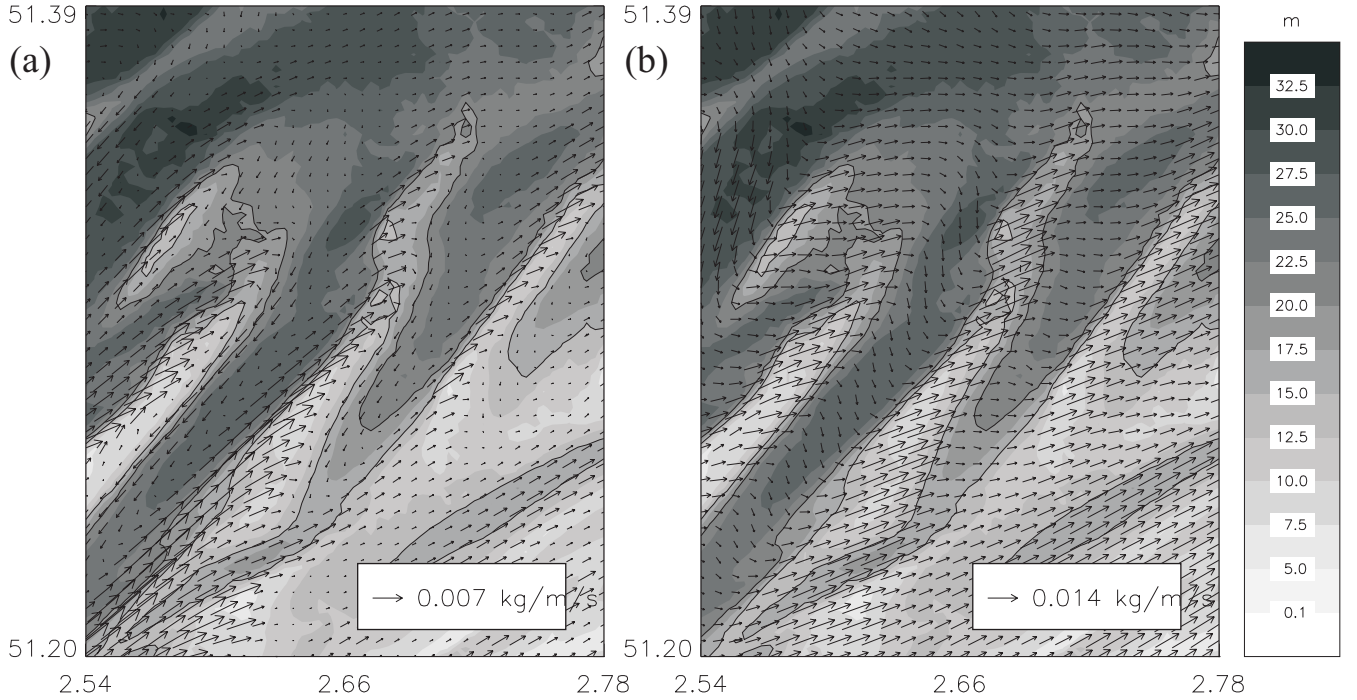

Figure 14. Predicted tidally-induced sediment transport on the Kwinte Bank for the period March 2nd 2004 6h30 – March 17th 2004 0h00 for Scenario 3, decrease of the sandbank height above 15 m below MSL, by 10.8 %. In the background the bathymetry is shown. (a) Results of MU-SEDIM, with one vector for each four grid points shown. (b) Results of the SISYPHE model, with the results being on the same grid as the MU-SEDIM model. Bathymetric contours are the 15 m and the 20 m depth contours, below MSL, of the original bathymetry (Figure 2).

2D model. The model utilised a constant median grain-size of 250 μm.

The total solid transport rate was calculated by means of the Soulsby-Van Rijn formula (Soulsby, 1997), applied to the currents on horizontal and sloping beds:

$$\overrightarrow{Q_s} = \left(A_{sb} + A_{ss}\right)\vec{u}\left[u - u_{\mathrm{cr}}\right]^{2.4}\left(1 - 1.6\tan\beta\right) \quad (6)$$

$$A_{sb} = \frac{0.005h(D_{50}/h)^{1.2}}{\left[(s-1)gD_{50}\right]^{1.2}} \quad (7)$$

$$A_{ss} = \frac{0.012D_{50}D_*^{-0.6}}{\left[(s-1)gD_{50}\right]^{1.2}} \quad (8)$$

$$D_* = \left(\frac{g(s-1)}{\nu^2}\right)^{1/3} D_{50} \quad (9)$$

where A_{sb} is the bed load component, A_{ss} is the suspended load component, u_{cr} the critical entrainment velocity, ß the slope of bed in a streamwise direction (assumed equal to 0), D_* the non-dimensional diameter, z_0 the bed roughness length (assumed equal to 0.006 m) and ν is the kinematic viscosity of the water.

The formula is validated for conditions in which the bed is rippled. Detailed multibeam imagery confirms that this requirement is satisfied (Van Lancker *et al*., 2004).

Validation under the Influence of Tides Alone

By way of a reference run, a simulation was performed for the period March 2nd 2004 6h30 to March 17th 2004 00h00, comprising an entire spring-neap tidal cycle.

The results for the residual sediment transport under the influence of tides, calculated with the MU-SEDIM model, are presented in Figure 7a. They are comparable with the results of a sediment transport model, based upon a two-dimensional hydrodynamic model, presented in Van Lancker *et al*. (2004). On the steep western side of the bank, sand transport is towards the northeast, whilst on the gently sloping eastern side, transport is in the ebb direction, *i.e*., towards the southwest. On the western side, the transport directions on the top of the bank veer to an almost perpendicular orientation, with respect to the banks' crest. This pattern is in agreement with the concept presented by Caston and Stride (1970), who described opposing sediment transport directions on either sides of a tidal sandbank; this is caused by an amplification of currents over the sandbank. The sediment transport rate is greatest on the top of the sandbank but much less in the swales. These results are similar to those of Brière *et al*. (this volume).

The results obtained with the SISYPHE model for the same period are presented in Figure 7b. The results show a dominant residual sediment transport, under the influence of tides alone, towards the northeast. Sediment transport over the area is much more uniform (see above) and return transport towards the southwest is not present. In the MU-SEDIM results, sediment transport in the swales, to the west and east of the Kwinte Bank, is towards the southwest. However, in the SISYPHE model results, transport is towards the southeast on the west of the bank; it is towards the east on the east. Furthermore, the rates predicted by the SISYPHE model are a factor of two larger than those of the MU-SEDIM model. Such differences are common in sediment transport modelling; Soulsby (1997) mentions that, in the sea, the total load sediment transport formulae give predictions within a factor of 5 in 70 % of the cases.

In order to validate the results of the models, the sediment transport patterns have been compared with these from dune asymmetries. As Lanckneus, De Moor, and Stolk, 1994, and Lanckneus *et al*. (2001) have shown, both the small to medium dune asymmetries and the large dune asymmetries can be used to derive sediment transport directions. Such asymmetry is, in the first place, defined by the dominant tidal current (Lanckneus *et al*., 2001). Further, although hydro-meteorological conditions, including the influence of waves, can alter the asymmetry of the bed forms, they return to their original tidally induced asymmetry, once a storm has abated. Therefore, it can be assumed that dune asymmetries, induced by tidal currents, can be used to validate model results for tides. Elsewhere, for the Kwinte Bank, Roche, Degrendele and Schotte, (2004) have presented sediment transport pathways, derived on the basis of dune asymmetries; they showed very similar patterns to those predicted by numerical models, *i.e*., residual sand transport on the steep western side of the bank in the direction of the flood currents, towards the northeast, whilst on the more gentle sloping eastern side of the bank, where ebb currents are dominant, southwesterly directed sediment transport occurs. Investigations undertaken within the context of the present study also confirm this pattern (Bellec *et al*., this volume).

Erosion and sedimentation patterns, derived from the simulated sediment transport, are presented in Figure 8a for the MU-SEDIM results. The Figure shows that under calm weather conditions, *i.e*., without taking into account the meteorological conditions and waves, erosion occurs on the steep western side of the sandbank; on the more gently sloping eastern side, some sand deposition may occur. Also on the top of the sandbank, some sand deposition occurs, tending to make the sandbank shallower. This interpretation is in agreement with the results obtained in the EU-MAST RESECUSED project (De Moor and Lanckneus, 1993). Here, it was shown that under calm weather conditions, the up-slope movement of sand under the influence of near-bed currents caused an accumulation of sand; under stormy conditions, the down-slope dispersion of sand results in a decrease in the volume of the upper part of the bank. The erosion and sedimentation patterns calculated with the SISYPHE model (Figure 8b) are, despite the differences in sediment transport rates, similar to the MU-SEDIM results. However, to the north and to the south of the bank, the area of erosion seems to be more extensive.

SIMULATION OF DIFFERENT SCENARIOS

The effect of large-scale sand extraction on the sediment transport and the morphodynamical evolution of the Kwinte Bank have been investigated using the models described. Three different scenarios have been studied.

In a first scenario, it is assumed that the entire sandbank (the dotted area, Figure 2), an area of 19.4 km², is deepened to 15 m below MSL. This represents an extracted volume of 59.7 10^6 m³, or an averaged deepening of the area by 3.07 m; it is clear that this is an unrealistic 'worst-case' scenario.

The two other scenarios are more realistic, where an extraction volume of 6.4 10^6 m^3 is extracted. Compared with the present level of sand extraction (about 1.9 10^6 m^3 every year), this represents the amount of material that could be extracted in less than 4 years.

In the second scenario, it has been assumed that this amount is extracted in a trench of about 1 km to 2 km in length, located in the area of the sandbank shallower than 13 m below MSL between 51.2604°N and 51.2697°N. A mean deepening of 3.11 m is established, with a maximum deepening of 5.40 m. These values are of the same order of magnitude as the deepening within the Central Depression.

In the last scenario, the same amount of material is extracted, but now over the entire area of the bank shallower than 15 m below MSL (dotted area, Figure 2). In all grid cells of this area, a proportion of material, 10.8 %, is extracted, relative to the sand available above the 15 m below MSL level. As a result, the mean water depth of the area is increased by 0.33 m in this case, with a maximum deepening at the top of the bank of 0.81 m.

Whilst both of the last scenarios are realistic in terms of the amount of material extracted, they represent the two possible ways of extraction: extraction from a specific area; or extraction over a much larger area.

Scenario 1: the 'Worst-Case' Scenario, Removing the Sandbank at 15 m below MSL

The new bathymetry of Scenario 1 is shown in Figure 9a. The effect on the sediment transport is considerable, as is shown by the results of the MU-SEDIM model (Figure 10a). The transport of sediment on the western side of the sandbank is significantly lower. Overall, the magnitude of the tidal-residual sediment transport, in the area where the bathymetry changed, decreased to 72 % of the original size. At the top of the sandbank, the sediment transport rate even decreased to only 28 % of the original transport rate. Furthermore, the returning transport to the southeast of the bank has almost disappeared. Similar results are presented by the SISYPHE model (Figure 10b), where the main effect is a decrease in the sediment transport rates over the Kwinte Bank. In this model, the rate of sediment transport on the top of the bank decreased to 45 % of the original.

The resulting morphodynamical changes are shown in Figure 11a, for the MU-SEDIM model results, and Figure 11b, for the SISYPHE results. It can be observed that for the MU-SEDIM model results, erosion on the western side of the bank decreased. Only on the northwestern side of the bank, near the kink, some erosion still occurs. Overall, on the bank itself, minor deposition is observed.

Minor deposition observed on the top of the sandbank appears to indicate that some regeneration mechanism could exist, to rebuild the sandbank, although the model results are not conclusive. Furthermore, it should be realised that the deposition rate is moderate; as such a regeneration of the sandbank would take a considerable amount of time. Furthermore, it is important to emphasise that, although the model results indicate a potential for regeneration, this does not indicate that the bank will regenerate. Such regeneration depends also upon the possible sources of new sand; this is not taken into account in the model.

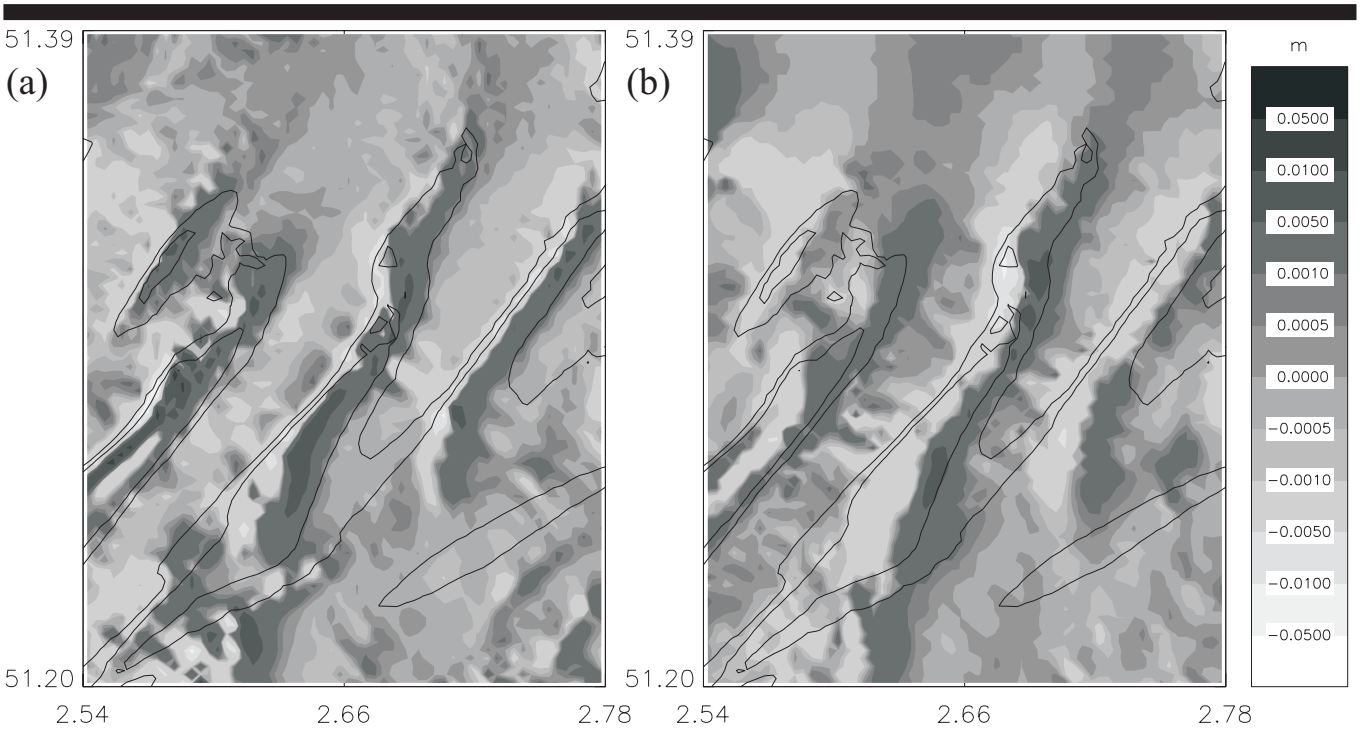

Figure 15. Erosion (light) and sedimentation (dark) patterns on the Kwinte Bank with tides only, for the period March 2nd 2004 6h30 – March 17th 2004 0h00 and for Scenario 3, decrease of the sandbank height above 15 m below MSL by 10.8 %. (a) Results of the MU-SEDIM model. (b) Results of the SISYPHE model. Bathymetric contours are shown for 15 m and 20 m below MSL.

Scenario 2: Moderate extraction from a specific area

In the Scenario 2, a more realistic amount of material is extracted from an area of approximately 1 km by 2 km, resulting in an overall deepening of the area of more than 3 m. The Scenario 2 bathymetry is shown in Figure 9b.

Whilst the main pattern of the sediment transport around the sandbank remains the same (see above), the effect of the trench cut in the sandbank can be identified on a local basis (Figure 12). The sediment transport rate decreases near and over the trench, whilst transport is directed slightly towards the direction of the trench. This decrease in sediment transport rate is reliant upon the combined effect of a decrease of the current over the trench and the increasing water depth; this results in a reduction of bottom stress. In the SISYPHE model, the influence of bathymetry on the sediment transport rate appears to be less pronounced. A reduction in the sediment transport rate over the trench is 78 % of the original. In the MU-SEDIM model results, the transport in the trench is reduced even further, to only 37 % of the original.

The effects on the morphodynamical changes are shown in Figure 13a, for the MU-SEDIM model. Erosion to the western side of the trench disappears, although to the north of the trench a small area of erosion is generated. Over most of the trench, moderate deposition occurs; however, this is smaller than the deposition on the eastern side of the bank. Such simulation appears to indicate that no breakthrough of the bank is developing, *i.e.,* that the trench has the tendency of infilling slowly. Again the SISYPHE model results show a similar trend (Figure 13b). Nevertheless, further research is required to be able to establish the existence of a regeneration mechanism.

Scenario 3: Moderate extraction over a larger area

In the last Scenario, the height of the sandbank, above 15 m below MSL (dotted area, Figure 2) has been decreased by 10.8 %. This results in an overall increase of the water depth over the entire area with only 0.3 m, but causes disturbance to a much larger area. The Scenario 3 bathymetry is shown in Figure 9c.

As could be expected, the sediment transport pattern (Figure 14) and the bottom evolution (Figure 15) are very similar to the situations associated with the original bathymetry. Here, also, clockwise sediment transport is found around the sandbank. Erosion takes place on the steep western side of the bank with deposition on the gently sloping eastern side of the bank. The sediment transport rate decreased on the top of the sandbank slightly to 83 % (95 %) of the original sediment transport for the MU-SEDIM (SISYPHE) model. Likewise erosion and deposition rates are somewhat lower than in the case of the original bathymetry. The simulation appears to indicate that regeneration is more probable, compared to the previous scenario, *i.e.*, with a trench.

DISCUSSION: INFLUENCE OF METEOROLOGICAL CONDITIONS AND WAVES

Introduction

In the previous Section of the paper, sediment transport over the Kwinte Bank was discussed under the influence of the tides alone. Different scenarios were simulated to investigate the influence of bathymetric changes on the sediment transport rates and directions. In this Section, the influence of the meteorological conditions and the waves on the sediment transport is discussed briefly. Firstly, two third-generation wave models are presented. Likewise, the modification to the sediment transport models, to include the wave effects, is discussed. Further, sediment transport under the influence of tides, prevailing meteorological conditions and waves is presented, for the same period as for the tide-only simulations.

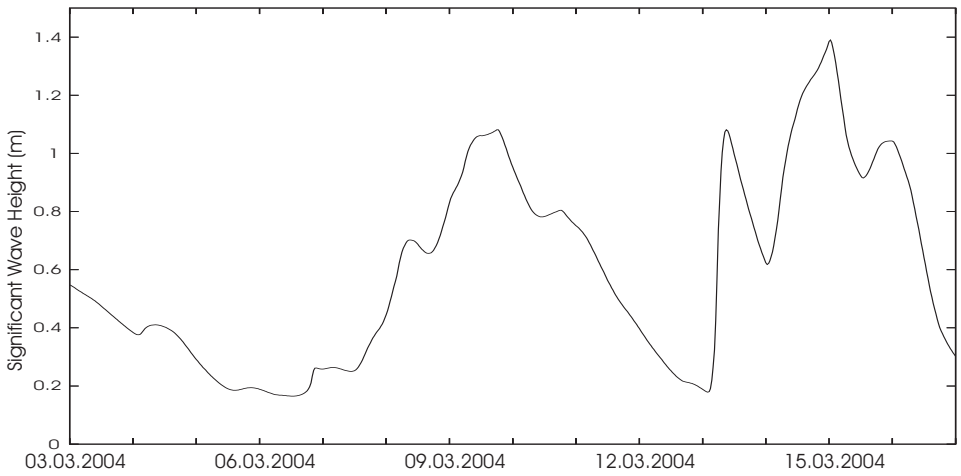

Figure 16. Significant wave height on the Kwinte Bank for the period March 2nd till March 17th 2004, as simulated by the TOMAWAC model.

Wave Models

Wave modelling was carried out using two different third-generation wave models: the WAM model (WAMDI, 1988), adapted for high-spatial resolution applications in shallow waters in the WAM-PRO version (Monbaliu *et al*., 2000); and the TOMAWAC model (Benoît, Marcos and Becq, 1996).

The WAM model solves the wave transport equation without any assumption in relation to the spectral shape. The physics of the wave evolution are represented for the full set of degrees of freedom, of a two-dimensional wave spectrum. The propagation and source terms are computed with different numerical methods and time-steps. The model was implemented on four nested model grids.

The TOMAWAC model (v.5.5) was implemented on the same mesh used by the hydrodynamic model TELEMAC-2D and the morphodynamical model SISYPHE. The model solves the balance equation of the wave action density spectrum and provides, to the SISYPHE model, the significant wave height, the peak period and the mean wave direction. More information on the TOMAWAC model can be found in Benoît, Marcos and Becq, (1996).

At the open sea boundaries, the wave models use a parametric JONSWAP spectrum for incoming waves, together with a complete wave absorption for outgoing waves.

The two wave models adopt a same spectral discretisation, with 12 directions and 25 frequencies. Source terms include input from the wind, bottom friction dissipation, white-capping and non-linear quadruple interactions (Monbaliu *et al*., 2000; Benoît, Marcos and Becq, 1996). Comparison of the two model performances, with buoy measurements, provide similar results in terms of significant wave height hindcasting with an average root-mean-square error of 0.25 m (Van Lancker *et al*., 2005).

Adaptations to the sediment transport models, to include the effect of waves

To account for the influence of the waves on the derivation of sediment transport pathways, using the 'total load' formula of Ackers and White (1973) in the MU-SEDIM model (see above), the friction velocity under the influence of currents and waves u_{*cw} has to be utilised, *i.e*., instead of the friction velocity under the influence of currents alone. In the MU-SEDIM model, the calculation of the bottom stress and the related friction velocity (Eq. 3), under the influence of currents and waves, is based upon the formula of Bijker (1966). Furthermore, the critical sediment mobility parameter *A* has been adapted by Swart (1976, 1977, *in*: Sleath, 1984), to include the effects of waves on sediment transport.

In order to include the effect of the waves on the total solid transport rate, as calculated by the Soulsby-Van Rijn formula (Soulsby, 1997), which is used in the SISYPHE model, a term is added in the equation, which is dependent upon the RMS orbital velocity of the waves at the bottom U_0 :

$$Q_{bs} = A_s U\left[\left(U^2 + 2\frac{0.018}{C_D}U_0^2\right)^{0.5} - U_{cr}\right]^{2.4}\left(1 - 1.6\tan\beta\right) \quad (9)$$

$$C_D = \left[\frac{0.40}{\ln(h/z_o) - 1}\right]^2 \quad (10)$$

with C_D being the drag coefficient due to currents alone.

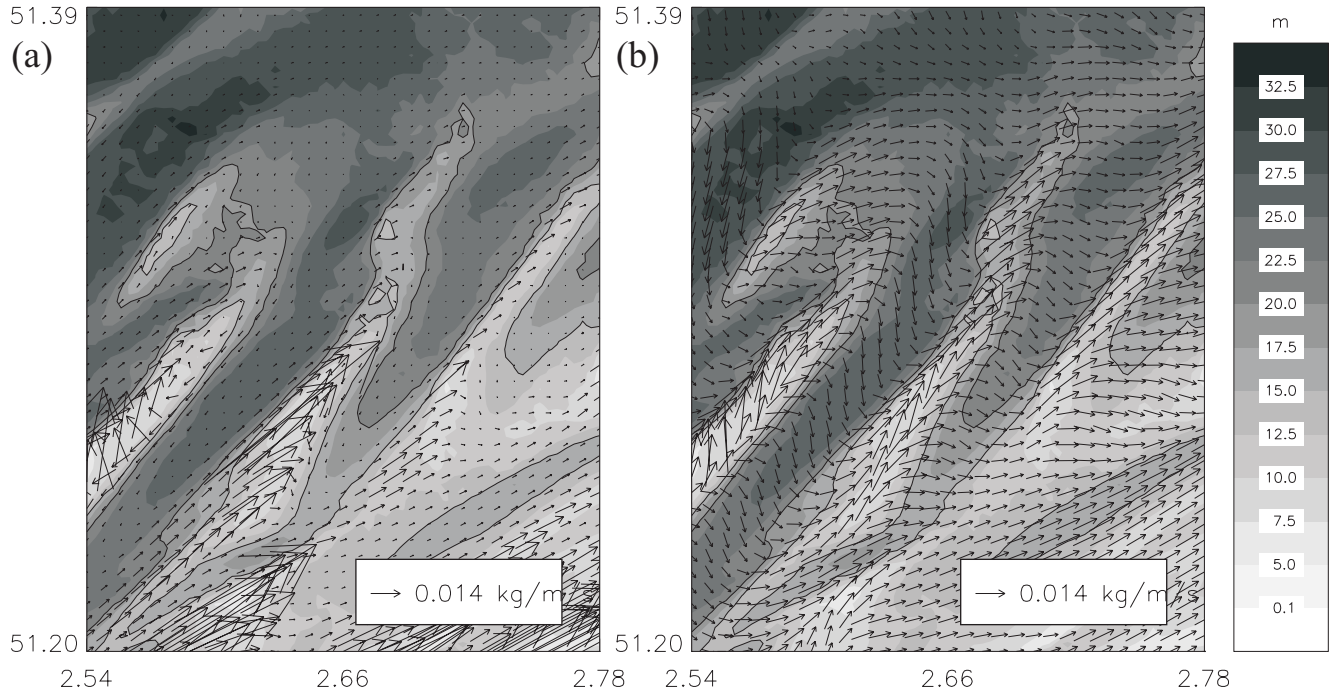

Figure 17. Predicted sediment transport under the influence of tides, meteorological conditions and waves, for the period March 2nd 2004 6h30 – March 17th 2004 0h00. In the background the bathymetry is shown. (a) Results of MU-SEDIM, with one vector for each four grid points shown. (b) Results of the SISYPHE model, with the results being on the same grid as the MU-SEDIM model. Bathymetric contours are the 15 m and the 20 m depth contours, below MSL, of the original bathymetry (Figure 2).

Sediment Transport under the Influence of Tides, Prevailing Meteorological Conditions and Waves

The simulation of sediment transport under the influence of tides, prevailing meteorological conditions and waves has been established for the same period, *i.e.,* from March 2nd 2004 6h30 to March 17th 2004 00h00. Over the selected period, selected waves over the Kwinte Bank reach a maximum of 1.4 m in height. The wave hindcasts from the TOMAWAC model are shown in Figure 16.

As shown in Figure 17a, sediment transport rates, calculated by the MU-SEDIM model, are clearly higher, when the waves are taken into account, especially in the shallower water areas (compare to Figure 7a). In such areas, where the water depth is less than 10 m below MSL, wave effects are important, modifying sediment transport under normal tidal conditions.

The enhancement of the sediment transport rates under the influence of waves, derived using the SISYPHE model (Figure 17b), is clearly smaller than the enhancement in the MU-SEDIM results (compare to Figures 17a and 7b). Whilst the transport of sediment under the influence of the tidally-only situation was mainly towards the northeast, the sediment transport under the influence of tides and waves, for this period, changed the directions to a more northerly direction.

From the above synthesis, it is evident that waves can have an important influence on sediment transport, even under moderate conditions; this will be investigated further in Giardino, Van den Eynde and Monbaliu, (this volume).

CONCLUSIONS

In the present contribution, the influence of bathymetric changes, in response to intense sand extraction, on erosional and depositional patterns on the Kwinte Bank, has been studied using numerical modelling. On the basis of the results obtained, an initial impression of the effect of sand extraction on the stability of the sandbank has been obtained.

Initially, the present situation was simulated, using sediment transport models. Using the MU-SEDIM model, a clockwise sediment transport pattern was found around the sandbank, with sediment transport towards the northeast on the steep western side of the sandbank and to the southwest on its gently sloping eastern side. Overall, this results in erosion on the western side and deposition on the eastern side, associated with a minor increase in height of the sandbank. This pattern is in agreement with the general view of transport around a sandbank under calm weather conditions, with an upslope movement of sand under the influence of tidally-induced near-bed currents causing an up-piling of sand (*e.g.*, De Moor and Lanckneus, 1993). The sediment transport patterns agree well with the directions derived from the asymmetries of the bed forms.

Three different scenarios were investigated, related to the amount and intensity of dredging. In the first scenario, the sandbank was removed at 15 m below MSL, representing a 'worst-case' scenario. A second, more realistic, scenario assumes a trench to be dredged, perpendicular to the crest of the sandbank, where an average deepening of about 3 m is established. In the last scenario, the same amount of material is extracted, but now over a much larger area.

The results of the simulations show that the intense sand extraction does not appear to affect the stability of the sandbank. Whilst there is less erosion and deposition after the sand extraction, a regeneration mechanism seems to be present, potentially allowing the sandbank to rebuild. Likewise, the trench created perpendicular to the crest of the sandbank seems be slowly refilled again. However, further research is needed to be able to make conclusive statements regarding the existence of a regeneration mechanism. In the case of the overall decrease of the sandbank above 15 m below MSL by 10.8 %, the sediment transport pattern is very similar to that obtained with the original bathymetry. Regeneration seems to be more probable for this scenario, compared to that of a trench with the same dredged volume.

These results are in agreement with those of Degrendele, Roche and Schotte, 2005, and Degrendele *et al.* (this volume). On the basis of intensive bathymetric monitoring, these investigations show, at least in the short-term, that, after the cessation of extraction in the Central Depression, the situation remained stable. No further erosion or no regeneration was apparent.

It is clear that deposition on the sandbank is very moderate and that, if regeneration of the sandbank is to occur, this will take a considerable amount of time. Following extensive sand extraction, resulting in significant lowering of the sandbank, the equilibrium height of the sandbank as it is at the present could be reached only again on a very long time-scale. Furthermore, it is important to realise that, although the model results indicate a potential for regeneration, regeneration of the sandbank depends also upon possible sources of new sand. This is not guaranteed.

Some preliminary results on the effects on the morphology of the sandbank are presented here. However, the sediment transport models used are still subject to important uncertainties. Further, it was shown that the effects of waves on the transport patterns and rates could be important; their effects, on the stability of the sandbank, are not investigated here. Nevertheless, some indications are provided that the stability of the sandbanks will not be affected dramatically as a result of the extraction of sand.

ACKNOWLEDGMENTS

This research was supported financially from the fees paid by the holders of licenses, for marine sand exploitation, issued by the Belgian authorities. The study was undertaken within the research objectives of the project MAREBASSE "Management, Research and Budgeting of Aggregates in Shelf Seas, related to End-users", supported by the Belgian Federal Office, PODOII programme (Contract No. EV/02/18A). The Captain and the crew of the R.V. *Belgica* are thanked for their flexibility and assistance, during the various campaigns. Michael Collins, Rik Houthuys and an anonymous reviewer are acknowledged for their constructive remarks.

LITERATURE CITED

Ackers, P. and White, W.R., 1973. Sediment transport: new approach and analysis. *Proceedings of the ASCE Journal of Hydraulics Division*, 99(HY11), 2041-2060.

Bellec, V.; Van Lancker, V.; Degrendele, K.; Roche, M., and Le Bot. S., this volume. Geo-environmental characterization of the Kwinte Bank. *Journal of Coastal Research*.

Benoît, M.; Marcos, F., and Becq, F., 1996. Development of a third generation shallow-water wave model with unstructured spatial meshing. *Proceedings of the 25th International Conference on Coastal Engineering* (Orlando, Florida, USA, American Society of Civil Engineers (ASCE)), pp. 465-478.

Bijker, E.W., 1966. The increase of bed shear in a current due to wave motion. *Proceedings of the 10th Conference on Coastal Engineering* (Tokyo, Japan, American Society of Civil Engineers (ASCE)), pp. 746-765.

Boyd, S.E.; Cooper, K.M.; Limpenny, D.S.; Kilbride, R.; Rees, H.L.; Dearnaley, M.P.; Stevenson, J.; Meadows, W.J., and Morris, C.D., 2004. Assessment of the re-habilitation of the seabed following marine aggregate dredging. Science Series, *Technical Report No. 121*, The Centre for Environment, Fisheries and Aquaculture Science & HR Wallingford, 154 p.

Brière, C.; Roos, P.; Garel, E., and Hulscher, S., this volume. Modeling the morphodynamic effects of sand extraction from the Kwinte Bank. *Journal of Coastal Research*.

Caston, V.N.D. and Stride, A.H., 1970. Tidal sand movement between some linear sandbanks in the North Sea off northeast Norfolk. *Marine Geology*, 9, M38-M42.

Cooreman, K.; Hillewaert, H.; Guns, M., and Van Hoeyweghen, P., 2000. Biological monitoring of dumping of dredged material at the Belgian coast (1997-1999) (in Dutch). Ministerie van Middenstand en Landbouw, Departement Zeevisserij, Oostende*, Report 97060/BAG/5*, 100 pp.

Degrendele, K.; Roche, M., and Schotte, P., 2002. Synthesis of data acquired from November 1999 to April 2001 concerning the extraction activities on the Kwintebank (in French). *Technical Report*, Fund for Sand Extraction, Ministry of Economic Affairs, 23 pp.

Degrendele, K.; Roche, M., and Schotte, P., 2005. Monitoring of the impact of the extraction (in Dutch). *Proceedings of the Workshop "Evaluation of the sustainable development of the sand and gravel extraction on the Belgian Continental Shelf and future perspectives",* (Oostende),1 p.

Degrendele, K.; Roche, M.; Schotte, P.; Van Lancker, V.; Bellec, V., and Bonne, W., this volume. Morphological evolution of the Kwinte Bank central depression before and after cessation of aggregate extraction. *Journal of Coastal Research*.

Deleu, S.; Van Lancker, V.; Van den Eynde, D., and Moerkerke, G., 2004. Morphodynamic evolution of the kink of an offshore tidal sandbank: the Westhinder Bank (Southern North Sea). *Continental Shelf Research*, 24, 1587-1610.

De Moor, G. and Lanckneus, J., (eds.), 1993. Sediment Mobility and Morphodynamics of the Middelkerke Bank. *Final Report MAST Project-0025-C RESECUSED*, Relation between Seafloor Currents and Sediment Mobility in the Southern North Sea. Universiteit Gent, 244 p.

Djenidi, S. and Ronday, F., 1992. Dynamique sédimentaire en mer à marée. *Etude du plateau continental nord-ouest Européen: Structure et mouvement verticaux*. Institut de recherches marines et d'interactions air-mer. Université de Liège, pp. 53-61.

Engelund, F.A. and Hansen, E., 1967. A monograph on sediment transport in alluvial streams. *Teknikal Forlag*, Copenhagen.

Fettweis, M. and Van den Eynde, D., 2000. Assessment of the sediment balance for the Belgian coastal waters: calculation with sediment transport models (in Dutch). Management Unit of the North Sea Mathematical Models*, Report SEBAB/1/MF/200006/NL/AR/2,* 45 pp.

Flather, R.A., 1981. Results From a Model of the North East Atlantic relating to the Norwegian Coastal Current. *In*: Saestre, R. and Mork, M. (eds.), *Proceedings of the Norwegian Coastal Current Symposium*, Geilo, pp.427-458.

Giardino, A. and Monbaliu, J., 2004. Tidal simulation in the North Sea - Code changes to TELEMAC-2D, Hydraulics Department KULeuven, *Internal Report*, 83 p.

Giardino, A.; Van den Eynde, D., and Monbaliu, J., this volume. Wave Effects on the Morphodynamic Evolution of an Offshore Sandbank. *Journal of Coastal Research*.

Grant, W.D. and Madsen, O.S., 1982. Movable bed roughness in unsteady oscillatory flow. *Journal of Geophysical Research*, 87, 469-481.

Hervouet, J.-M. and Bates, P., 2000, The TELEMAC Modelling System. Special Issue, *Hydrological Processes*, 14, Baffins Lane, West Sussex PO19 1UD, United Kingdom, John Wiley & Sons Ltd., 2207-2363.

Hoogewoning, S.E. and Boers, M., 2001. Physical effects of marine sand extraction (in Dutch). *Rapport RIKZ/2001.050*, Rijkswaterstaat, 95 p.

ICES, 2005. WGEXT Report 2003. ICES Marine Habitat Committee, *ICES Report,* CM 2005/E:06.

Lanckneus, J.; De Moor, G., and Stolk, A., 1994. Environmental setting, morphology and volumetric evolution of the Middelkerke Bank (Southern North Sea). *Marine Geology*, 121, 1-21.

Lanckneus, J.; Van Lancker, V.; Moerkerke, G.; Van den Eynde, D.; Fettweis, M.; De Batist, M., and Jacobs, P., 2001. Investigation of the natural sand transport on the Belgian Continental Shelf (BUDGET). *Final Report*. Federal Office for Scientific, Technical and Cultural Affairs (OSTC), 104 p. + 87 p.

Luyten, P.J.; Jones, J.E.; Proctor, R.; Tabor, A.; Tett, P., and Wild-Allen, K., 1999. COHERENS: A Coupled Hydrodynamical-Ecological Model for Regional and Shelf Seas: User Documentation. *Technical Report*, Management Unit of the North Sea Mathematical Models, Brussels, 914 p.

Monbaliu, J.; Padilla-Hernandez, R.; Hargreaves, J.C.; Albiach, J.C.C.; Luo, W.; Sclavo, M., and Günther, H., 2000, The spectral wave model, WAM, adapted for applications with high spatial resolution, *Journal of Coastal Engineering*, 41 (1-3), 41-62.

Pison, V. and Ozer, J., 2003. Operational products and services for Belgian coastal waters. *In:* Dahlin, H.; Flemming, N.C.; Nittis K., and Peterson, S.E. (eds.), *Building the European Capacity in Operational Oceanography. Proceedings of the Third International Conference on EuroGOOS*. Elsevier Oceanography Series, 69, 503-509.

Roche, M.; Degrendele, K., and Schotte, P., 2004. Introduction to the Kwinte Bank from a geomorphological perspective. Fund for Sand Extraction, Ministry of Economic Affairs. *Presentation on the SPEEK Workshop*, Gent.

Sleath, J.F.A., 1984. *Sea Bed Mechanics*. New York: Wiley-Interscience, 335 p.

Soulsby, R.L., 1997. *Dynamic of Marine Sands*. London: Thomas Telford, 272 p.

Svašek, 2001. PUTMOR: field measurements at a temporary sand pit. Part 3: Final Report. *Report 01453/1177 Final*, 27 pp.

Swart, D.H., 1976. Coastal sediment transport. Computation of longshore transport. The Netherlands: Delft Hydraulics Laboratory, *Report R968* (1).

Swart, D.H., 1977. Weighted value of depth of initiation of movement. South Africa: Stellenbosch, *Report NR10*.

Van den Eynde, D. and Ozer, J., 1993. Sediment Trend Analysis: calculation of the sediment transport with a numerical model (in Dutch). Management Unit of the North Sea Mathematical Models, *Rapport BMM/STA/TR01*, 49 pp.

Van den Eynde, D.; Scory, S., and Malisse, J.-P., 1995. Operational modelling of tides and waves in the North Sea on the Convex C230 at MUMM. *Proceedings of the European Convex User's Conference 1995* (Brussels, Belgium).

Van Lancker, V.; Deleu, S.; Bellec, V.; Le Bot, S.; Verfaillie, E.; Fettweis, M.; Van den Eynde, D.; Francken, F.; Pison, V.; Wartel, S.; Monbaliu, J.; Portilla, J.; Lanckneus, J.; Moerkerke, G., and Degraer, S., 2004. Management, research and budgeting of aggregates in shelf seas related to end-users (Marebasse). *Scientific Report*, Year 2. Federal Office of Scientific, Technical and Cultural Affairs (OSTC), 144 p.

Van Lancker, V.; Deleu, S.; Bellec, V.; Du Four, I. ; Verfaillie, E.; Fettweis, M.; Van den Eynde, D.; Francken, F.; Monbaliu, J.; Giardino, A.; Portilla, J.; Lanckneus, J.; Moerkerke, G., and Degraer, S., 2005. Management, research and budgeting of aggregates in shelf seas related to end-users (Marebasse). *Scientific Report*, Year 3. Federal Office of Scientific, Technical and Cultural Affairs (OSTC), 103 pp.

Villaret, C., 2004. SISYPHE release 5.4. *User Manual*. EDF/LNHE, Chateau France. 69p.

WAMDI group., 1988. The WAM model - a third generation ocean wave prediction model, *Journal of Physical Oceanography*, 18, 1775-1810.

Yu, C.S.; Vermunicht, A.; Rosso, M.; Fettweis, M., and Berlamont, J., 1990. Numerical simulation of long waves on the north-west European Continental Shelf. Part 2: Model setup and calibration. Belgium: Katholieke Universiteit Leuven, *Technical Report BH/88/28*.